Available online at www.sciencedirect.com
SCIENCE DIRECT®
Computer Vision and Image Understanding 97 (2005) 86–102
Computer Vision and Image Understanding
www.elsevier.com/locate/cviu

The geometric error for homographies☆

Ondřej Chum,[a,*] Tomáš Pajdla,[a] and Peter Sturm[b]

[a] *Center for Machine Perception, Department of Cybernetics, Czech Technical University in Prague, Faculty of Electrical Engineering, Karlovo náměstí 13, 121 35 Praha 2, Czech Republic*
[b] *INRIA Rhône-Alpes, 655 Avenue de l'Europe, Montbonnot 38330, France*

Received 23 July 2003; accepted 10 March 2004
Available online 22 April 2004

Abstract

We address the problem of finding optimal point correspondences between images related by a homography: given a homography and a pair of matching points, determine a pair of points that are exactly consistent with the homography and that minimize the geometric distance to the given points. This problem is tightly linked to the triangulation problem, i.e., the optimal 3D reconstruction of points from image pairs. Our problem is non-linear and iterative optimization methods may fall into local minima. In this paper, we show how the problem can be reduced to the solution of a polynomial of degree eight in a single variable, which can be computed numerically. Local minima are thus explicitly modeled and can be avoided. An application where this method significantly improves reconstruction accuracy is discussed. Besides the general case of homographies, we also examine the case of affine transformations, and closely study the relationships between the geometric error and the commonly used Sampson's error, its first order approximation. Experimental results comparing the geometric error with its approximation by Sampson's error are presented.

Keywords: Homography; Geometric error; Sampson's error; Triangulation

☆ The authors were supported by Grants GACR 102/01/0971, FP5 EU IST-2001-39184, Aktion 34p24, MSM 212300013, CTU0306013, and STINT Dur IG2003-2 062. We thank Mirko Navara for helping us with the proofs.

* Corresponding author.
E-mail addresses: chum@cmp.felk.cvut.cz (O. Chum), pajdla@cmp.felk.cvut.cz (T. Pajdla), Peter.Sturm@inrialpes.fr (P. Sturm).

1077-3142/$ - see front matter
doi:10.1016/j.cviu.2004.03.004

1. Introduction

Homographies are used in many applications, e.g., in mosaicing [1] or wide baseline stereo matching [2,3]. In many applications we also need to compute the error (or the distance) of a point correspondence with respect to a given homography $\mathtt{H}$. This is necessary for instance in RANSAC [4], a commonly used robust estimation algorithm. Some applications may require not only to compute the distance of a given point correspondence to the model of homography but actually need to determine points, which are consistent with the given homography and are in a small neighborhood of the measured, thus noisy, given points.

This work addresses the problem of finding optimal point correspondences between images related by an homography: given a known homography and a pair of matching noisy points, determine a pair of points that are exactly consistent with the homography and that minimize the geometric distance to the given noisy points. There are two approaches to achieve such a goal [5]: (1) non-linear optimization using iterative methods and (2) parametric approach, where the solution is parametrized so that it automatically satisfies the given constraint. The paper concentrates on the latter strategy.

A similar problem, based on the geometric error for the epipolar geometry, has been addressed by Hartley and Sturm [6]. The geometric error for homographies was introduced by Sturm [7, Appendix B], and independently derived by Chum and Pajdla in [8,9]. In this paper, previous results are reviewed from a common perspective, the derivation of the geometric error for homographies is described and a mathematical proof of its correctness given. Furthermore, we discuss the commonly used approximation of the geometric error, Sampson's error. Links between the two are studied in detail, for the general case of homographies, as well as the case of affine transformations between images.

The rest of the paper is structured as follows. Basic concepts are introduced in Section 2. Section 3 contains the derivation of the formulae for the geometric error. In Section 4, Sampson's approximation is derived and studied. Geometric properties of both error measures are studied in Section 5. Experiments are presented in Section 6. An application of the proposed method is described in Section 7 and conclusions are given in Section 8.

2. Basic concepts

We assume that a planar homography $\mathtt{H}$ [10] and a noisy correspondence $\mathbf{x} \leftrightarrow \mathbf{x}'$ measured in the images are given. Let the homogeneous coordinates of the corresponding points be $\mathbf{x} = (x, y, 1)^{\mathrm{T}}$ and $\mathbf{x}' = (x', y', 1)^{\mathrm{T}}$ and the homography be represented by the (regular) matrix

$$\mathtt{H} = \begin{pmatrix} h_1 & h_2 & h_3 \\ h_4 & h_5 & h_6 \\ h_7 & h_8 & h_9 \end{pmatrix}.$$

There are several possible ways to measure the "error" of that point correspondence with respect to the homography. We will mention the geometric error and Sampson's approximation of it.

Supposing the Gaussian noise model for perturbations of image coordinates, the maximum likelihood estimation of the position of the noise-free correspondence $\hat{\mathbf{x}} \leftrightarrow \mathtt{H}\hat{\mathbf{x}}$ is obtained by minimizing the *geometric error* $d_{\perp}^2 = d(\mathbf{x}, \hat{\mathbf{x}})^2 + d(\mathbf{x}', \mathtt{H}\hat{\mathbf{x}})^2$ over all $\hat{\mathbf{x}}$ (Fig. 1). This error measure could be thought of as the Euclidean distance of point $\mathbf{X} = (x, y, x', y') \in \mathbb{R}^4$, representing the given point correspondence, to the two-dimensional variety $\mathcal{V}_{\mathtt{H}}$ (Fig. 2) defined as

$$\mathcal{V}_{\mathtt{H}} = \{\mathbf{Y} \in \mathbb{R}^4 \,|\, \mathbf{t}(\mathbf{Y}) = \mathbf{0}\}, \tag{1}$$

where $\mathbf{t} = (t_x, t_y)^{\mathrm{T}}$ and

$$t_x = Y_1 h_1 + Y_2 h_2 + h_3 - Y_1 Y_3 h_7 - Y_2 Y_3 h_8 - Y_3 h_9, \tag{2}$$

$$t_y = Y_1 h_4 + Y_2 h_5 + h_6 - Y_1 Y_4 h_7 - Y_2 Y_4 h_8 - Y_4 h_9, \tag{3}$$

i.e., such $\mathbf{Y}$ represent point correspondences that are consistent with $\mathtt{H}$.

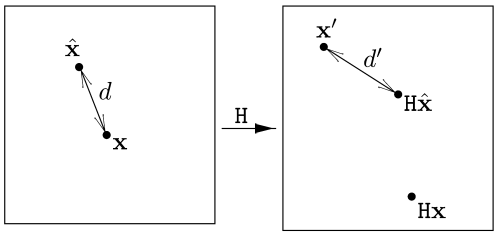

Fig. 1. Two images linked by homography $\mathtt{H}$. Points $\mathbf{x}$ and $\mathbf{x}'$ are measured points, $\hat{\mathbf{x}}$ is the point minimizing $d^2 + d'^2$ where d and d' are the distances $\mathbf{x}$ to $\hat{\mathbf{x}}$ and $\mathbf{x}'$ to $\mathtt{H}\hat{\mathbf{x}}$.

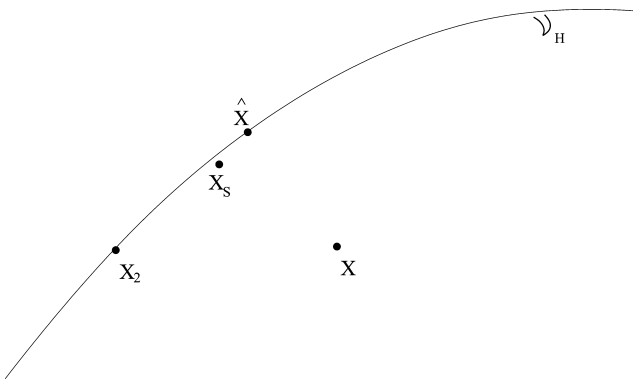

Fig. 2. The variety $\mathcal{V}_{\mathtt{H}}$ and points where different error measures of the measured noisy point correspondence $\mathbf{X}$ with respect to homography $\mathtt{H}$ are minimized. The geometric error is minimized at $\hat{\mathbf{X}}$, Sampson's error at $\mathbf{X}_{\mathrm{S}}$, and the error in the second image at $\mathbf{X}_2$.

The first-order approximation of this error measure, called *Sampson's error*, was first used by Sampson [11] for conics. The derivation of Sampson's error for homographies is described in Section 4.

The exact computation of the geometric error is equivalent to finding the point $\hat{\mathbf{X}} \in \mathbb{R}^4$ on the variety $\mathcal{V}_{\mathtt{H}}$, that minimizes the Euclidean distance to the measured point $\mathbf{X}$. We show that the geometric error can be exactly determined by solving a polynomial of degree eight.

3. The geometric error

In this section the problem of computing the geometric error is transformed, so that it reduces to finding roots of a polynomial of degree eight.

The distance of points lying on the variety $\mathcal{V}_{\mathtt{H}}$ to the measured point correspondence $\mathbf{X}$ can be written as a function of the matrix $\mathtt{H}$, the measured image points $\mathbf{x}$, $\mathbf{x}'$, and a point $\hat{\mathbf{x}}$ in the first image. If we expand the matrix multiplication, we have

$$e(\hat{\mathbf{x}}) = (x - \hat{x})^2 + (y - \hat{y})^2 + (x' - \hat{x}')^2 + (y' - \hat{y}')^2, \tag{4}$$

where

$$\hat{x}' = \frac{h_1\hat{x} + h_2\hat{y} + h_3}{h_7\hat{x} + h_8\hat{y} + h_9} \tag{5}$$

and

$$\hat{y}' = \frac{h_4\hat{x} + h_5\hat{y} + h_6}{h_7\hat{x} + h_8\hat{y} + h_9}. \tag{6}$$

Directly solving the equation $(\partial e/\partial \hat{y}) = 0$ leads to a polynomial in two variables of order four in $\hat{x}$ and order five in $\hat{y}$. The same happens for the partial derivative of e with respect to $\hat{x}$. Therefore, we first transform the images such as to lower the degree of the polynomial. We use Euclidean transformations, which do not change distances, and thus the solution of the transformed problem will be the transformed solution of the original problem.

At first we shift the points $\mathbf{x}$ and $\mathbf{x}'$ to the origin of the first and the second image, respectively. This is achieved by applying the following translations:

$$\mathtt{L} = \begin{pmatrix} 1 & 0 & -x \\ 0 & 1 & -y \\ 0 & 0 & 1 \end{pmatrix}, \quad \mathtt{L}' = \begin{pmatrix} 1 & 0 & -x' \\ 0 & 1 & -y' \\ 0 & 0 & 1 \end{pmatrix}.$$

After translating the images we have

$$\mathtt{L}'\hat{\mathbf{x}}' \sim \mathtt{L}'\mathtt{H}\mathtt{L}^{-1}\mathtt{L}\hat{\mathbf{x}}. \tag{7}$$

In this equation, $\sim$ stands for "equal up to a nonzero scale." Let $\mathtt{B} = \mathtt{L}'\mathtt{H}\mathtt{L}^{-1}$ be the homography between the transformed images and $\bar{\mathbf{x}} = \mathtt{L}\hat{\mathbf{x}}$. We can easily verify that

the first two entries in the third row of the matrix B equal the corresponding entries in $\mathtt{H}$ after applying the translations, and so

$$\mathtt{B} = \begin{pmatrix} b_1 & b_2 & b_3 \\ b_4 & b_5 & b_6 \\ h_7 & h_8 & b_9 \end{pmatrix}. \tag{8}$$

We can now rewrite (re-parameterize) the error term e as follows:[1]

$$e(\hat{\mathbf{x}}) = e(\bar{\mathbf{x}}) = \bar{x}^2 + \bar{y}^2 + \left(\frac{b_1\bar{x} + b_2\bar{y} + b_3}{h_7\bar{x} + h_8\bar{y} + b_9}\right)^2 + \left(\frac{b_4\bar{x} + b_5\bar{y} + b_6}{h_7\bar{x} + h_8\bar{y} + b_9}\right)^2. \tag{9}$$

From (9) we can observe, that solving for the minimum of e would be simple if h_8 were equal to 0, as $\partial e/\partial\bar{y}$ would be linear in $\bar{y}$ (e would be quadratic in $\bar{x}$). To achieve this situation, we simply rotate the first image appropriately: we design a rotation matrix $\mathtt{R}$ so that the homography between the rotated first image and the second image, i.e., $\mathtt{Q} = \mathtt{B}\mathtt{R}^{-1}$, satisfies $q_8 = 0$. With

$$\mathtt{R} = \begin{pmatrix} \cos(\alpha) & -\sin(\alpha) & 0 \\ \sin(\alpha) & \cos(\alpha) & 0 \\ 0 & 0 & 1 \end{pmatrix}$$

the rotation angle α for which $q_8 = h_7\sin(\alpha) + h_8\cos(\alpha) = 0$ is obtained as

$$\alpha = \arctan\left(-\frac{h_8}{h_7}\right). \tag{10}$$

Now we can rewrite the term e as follows:

$$e(\tilde{\mathbf{x}}) = \tilde{x}^2 + \tilde{y}^2 + \left(\frac{q_1\tilde{x} + q_2\tilde{y} + q_3}{q_7\tilde{x} + q_9}\right)^2 + \left(\frac{q_4\tilde{x} + q_5\tilde{y} + q_6}{q_7\tilde{x} + q_9}\right)^2, \tag{11}$$

where $\tilde{\mathbf{x}} = \mathtt{R}\bar{\mathbf{x}} = \mathtt{R}\mathtt{L}\hat{\mathbf{x}}$. The partial derivative $\partial e/\partial\tilde{y}$ is linear in $\tilde{y}$. The minimum is reached in $\partial e/\partial\tilde{y} = 0$, so

$$\tilde{y} = -\frac{q_2q_3 + q_5q_6 + q_1q_2\tilde{x} + q_4q_5\tilde{x}}{q_2^2 + q_5^2 + q_9^2 + 2q_7q_9\tilde{x} + q_7^2\tilde{x}^2}. \tag{12}$$

Now we can simply substitute (12) into (11) and find the minimum of e. Solving

$$\frac{\partial e}{\partial\tilde{x}}(\tilde{x}, \tilde{y}) = 0$$

gives a polynomial of degree eight which is completely given in Appendix B. The proof of correctness of the procedure described above, i.e., the proof that a global minimum of the function e *exists* and that the partial derivatives are *defined* at it, can be found in Appendix A.

[1] The function e is parametrized not only by $\hat{\mathbf{x}}$, but also by $\mathbf{x}$, $\mathbf{x}'$, and $\mathtt{H}$. The term $e(\hat{\mathbf{x}})$ actually stands for $e(\hat{\mathbf{x}}, \mathbf{x}, \mathbf{x}', \mathtt{H})$, whereas $e(\bar{\mathbf{x}})$ stands for $e(\bar{\mathbf{x}}, \mathtt{L}\mathbf{x}, \mathtt{L}'\mathbf{x}', \mathtt{B})$.

3.1. The affine case

Eqs. (2) and (3) are linear in the entries of the mapping matrix and bilinear in the entries of $\mathbf{Y}$ when a full homography matrix is sought.

Proposition 1. *Eqs.* (2) *and* (3) *are linear in the entries of* $\mathbf{Y}$ *if and only if the mapping is affine.*

Proof. If (and only if) both $h_7 = 0$ and $h_8 = 0$, then (2) and (3) are linear in the entries of $\mathbf{Y}$. This exactly corresponds to affine mappings. □

For an affine transformation, $\mathbf{x}' = \mathtt{A}\mathbf{x}$, where

$$\mathtt{A} = \begin{pmatrix} a_1 & a_2 & a_3 \\ a_4 & a_5 & a_6 \\ 0 & 0 & 1 \end{pmatrix},$$

the geometric error can be easily obtained in closed form. As the error function

$$e = (\hat{x} - x)^2 + (\hat{y} - y)^2 + (a_1\hat{x} + a_2\hat{y} + a_3 - y')^2 + (a_4\hat{x} + a_5\hat{y} + a_6 - y')^2$$

is order of two in both $\hat{x}$ and $\hat{y}$, partial derivatives $\partial e/\partial x$ and $\partial e/\partial \hat{y}$ are linear in both $\hat{x}$ and $\hat{y}$. Solving the system $\partial e/\partial \hat{x} = 0$ and $\partial e/\partial \hat{y} = 0$ using, e.g. [12] yields (in the general case) a unique solution

$$\begin{aligned} N &= (a_5^2 + 1)(a_1^2 + 1) - 2a_1a_2a_4a_5 + a_2^2 + a_2^2a_4^2 + a_4^2, \\ \hat{x} &= \frac{1}{N}\big(a_1(a_2a_5a_6 - a_3 - a_3a_5^2) + a_2a_3a_4a_5 - (a_4a_6)(a_2^2 + 1) + x(a_5^2 + a_2^2 + 1) \\ &\quad - y(a_1a_2 + a_4a_5) + x'(a_1 + a_1a_5^2 - a_2a_4a_5) + y'(a_4 - a_1a_2a_5 + a_2^2a_4)\big), \\ \hat{y} &= \frac{1}{N}\big(a_1(a_3a_4a_5 + a_2a_4a_6) - (a_5a_6)(a_1^2 + 1) - (a_2a_3)(a_4^2 + 1) - x(a_1a_2 + a_4a_5) \\ &\quad + y(a_1^2 + a_4^2 + 1) + x'(a_2 - a_1a_4a_5 + a_2a_4^2) + y'(a_5 - a_1a_2a_4 + a_1^2a_5)\big). \end{aligned}$$

4. Sampson's error

To find the closest point on the variety $\mathcal{V}_{\mathtt{H}}$ to our measured correspondence $\mathbf{x} \leftrightarrow \mathbf{x}'$, or $\mathbf{X} \in \mathbb{R}^4$, requires solving a polynomial of degree eight, which is computationally expensive. Another possibility is to compute an approximation of the geometric error.

We can use the first-order Taylor approximation of t_x and t_y by their tangent hyperplanes in the measured point $\mathbf{X}$. Let $\mathbf{J}$ be the Jacobian matrix

$$\mathbf{J}_{\mathtt{H},\mathbf{x},\mathbf{x}'} = \begin{pmatrix} \frac{\partial t_x(\mathbf{X})}{\partial x} & \frac{\partial t_x(\mathbf{X})}{\partial y} & \frac{\partial t_x(\mathbf{X})}{\partial x'} & \frac{\partial t_x(\mathbf{X})}{\partial y'} \\ \frac{\partial t_y(\mathbf{X})}{\partial x} & \frac{\partial t_y(\mathbf{X})}{\partial y} & \frac{\partial t_y(\mathbf{X})}{\partial x'} & \frac{\partial t_y(\mathbf{X})}{\partial y'} \end{pmatrix}.$$

To simplify $\mathbf{J}$ for further use, we apply the observations that $\frac{\partial t_x(\mathbf{X})}{\partial y'} = 0$, $\frac{\partial t_y(\mathbf{X})}{\partial x'} = 0$, and $\frac{\partial t_x(\mathbf{X})}{\partial x'} = \frac{\partial t_y(\mathbf{X})}{\partial y'}$. We obtain $\mathbf{J}$ in the following form:

$$\mathbf{J}_{\mathrm{H},\mathbf{x},\mathbf{x}'} = \mathbf{J} = \begin{pmatrix} j_1 & j_2 & j_3 & 0 \\ j_4 & j_5 & 0 & j_3 \end{pmatrix},$$

where $j_1 = h_1 - h_7x'$, $j_2 = h_2 - h_8x'$, $j_3 = -h_7x - h_8y - h_9$, $j_4 = h_4 - h_7y'$, and $j_5 = h_5 - h_8y'$ are the respective partial derivatives. Then, the first order Taylor approximation of $\mathbf{t}$ is

$$\tilde{\mathbf{t}}(\tilde{\mathbf{X}}) = \mathbf{t}(\mathbf{X}) + \mathbf{J}(\tilde{\mathbf{X}} - \mathbf{X}). \tag{13}$$

The approximate solution (Sampson's error) might be found as the closest point to $\mathbf{X}$ on the two-dimensional variety $\mathcal{V}_S$ defined as follows:

$$\mathcal{V}_S = \{\tilde{\mathbf{X}} \in \mathbb{R}^4 \mid \tilde{\mathbf{t}}(\tilde{\mathbf{X}}) = \mathbf{0}\}.$$

As $\mathcal{V}_S$ is linear, the solution is given by

$$\mathbf{X}_S = \mathbf{J}^+\mathbf{t}(\mathbf{X}) + \mathbf{X},$$

where $\mathbf{J}^+ = \mathbf{J}^{\mathrm{T}}(\mathbf{J}\mathbf{J}^{\mathrm{T}})^{-1}$ is the pseudo-inverse of the Jacobian $\mathbf{J}$.

If we have a closer look at the function $\tilde{\mathbf{t}}$ (Eq. (13)), we can observe that it is similar to the function $\mathbf{t}$, but linear in the entries of $\tilde{\mathbf{X}}$. If we examine it in more detail, we find that Sampson's error is in fact the geometric error for the affine transformation, that locally approximates the homography $\mathtt{H}$. The affine approximation $\mathbf{x}' = A_{\mathtt{H}}\mathbf{x}$ of the homography $\mathtt{H}$ in the measured points $\mathbf{x} \leftrightarrow \mathbf{x}'$ is as follows:

$$A_{\mathtt{H}} = \frac{1}{j_3}\begin{pmatrix} j_1 & j_2 & -j_1x - j_2y - j_3x' + t_x(\mathbf{X}) \\ j_4 & j_5 & -j_4x - j_5y - j_3y' + t_y(\mathbf{X}) \\ 0 & 0 & j_3 \end{pmatrix}.$$

The affine transformation $A_{\mathtt{H}}$ has the same partial derivatives as $\mathtt{H}$ in the measured point $\mathbf{X}$. Let us give a geometric interpretation of $A_{\mathtt{H}}$. The construction of $A_{\mathtt{H}}$ based on the points that are mapped identically by both, the homography $\mathtt{H}$ and its affine approximation $A_{\mathtt{H}}$, gives an illustrative explanation. These points are given as the fixed points of $A_{\mathtt{H}}^{-1}\mathtt{H}$. The eigenvectors and eigenvalues of $A_{\mathtt{H}}^{-1}\mathtt{H}$ are in the general case (using [12]) $\mathbf{v_1} = (h_8, -h_7, 0)^{\mathrm{T}}$, $\lambda_1 = 1$, $\mathbf{v_2} = (0, h_7x + h_8y, h_8)^{\mathrm{T}}$, $\lambda_2 = 1$, and $\mathbf{v_3} = \mathtt{H}^{-1}\mathbf{x}'$, $\lambda_3 \neq 1$. Hence, there is a line of fixed points, passing through the points $\mathbf{v_1}$ and $\mathbf{v_2}$ (including $\mathbf{x} = x\mathbf{v_1} + \mathbf{v_2}$) and a fixed point $\mathtt{H}^{-1}\mathbf{x}'$. The point $\mathbf{v_1}$ is the only point (in general) that is mapped by the non-affine homography from the line at infinity to the line at infinity, i.e., $\mathtt{H}^{-1}(\mathtt{H}^{-\mathrm{T}}(0,0,1)^{\mathrm{T}} \times (0,0,1)^{\mathrm{T}})$, satisfying $(h_7, h_8, h_9)\mathbf{v_1} = 0$.

5. Geometric properties

An important property of an error measure is its independence of the choice of the Cartesian coordinate system in the images. In this section, we study the behavior of

the discussed error measures under the application of rigid transformations to the images. The originally formulated relation $\mathbf{x}' \sim \mathtt{H}\mathbf{x}$ changes to

$$\mathtt{T}'\mathbf{x}' \sim (\mathtt{T}'\mathtt{H}\mathtt{T}^{-1})\mathtt{T}\mathbf{x},$$

where $\mathtt{T}$ and $\mathtt{T}'$ represent the rigid image transformations of the first and the second image, respectively.

As distances in the images are not affected by rigid transformations and the new homography links the transformed points, the geometric error remains the same. We already used this property in Section 3.

Proposition 2. *The Jacobian* $\mathbf{J}$ *is covariant to any affine transformation of the images. Let* $\mathtt{T}$ *and* $\mathtt{T}'$ *be affine transformations of the first and second image respectively, and* $\mathtt{H}_1$, $\mathtt{H}_2$ *be homographies satisfying* $\mathbf{J}_{\mathtt{H}_1,\mathbf{x},\mathbf{x}'} \sim \mathbf{J}_{\mathtt{H}_2,\mathbf{x},\mathbf{x}'}$. *Then* $\mathbf{J}_{\mathtt{T}'\mathtt{H}_1\mathtt{T}^{-1},\mathtt{T}\mathbf{x},\mathtt{T}'\mathbf{x}'} \sim \mathbf{J}_{\mathtt{T}'\mathtt{H}_2\mathtt{T}^{-1},\mathtt{T}\mathbf{x},\mathtt{T}'\mathbf{x}'}$.

Proof. Denote the affine transformations as

$$\mathtt{T} = \begin{pmatrix} t_1 & t_2 & t_3 \\ t_4 & t_5 & t_6 \\ 0 & 0 & 1 \end{pmatrix} \quad \text{and} \quad \mathtt{T}' = \begin{pmatrix} t'_1 & t'_2 & t'_3 \\ t'_4 & t'_5 & t'_6 \\ 0 & 0 & 1 \end{pmatrix}.$$

The Jacobian $\mathbf{J}$ after transforming the first and the second image, respectively can be expressed in terms of the transformations $\mathtt{T}$ and $\mathtt{T}'$ and the original Jacobian $\mathbf{J}$ as follows:

$$\mathbf{J}_{\mathtt{T}'\mathtt{H},\mathbf{x},\mathtt{T}'\mathbf{x}'} = \begin{pmatrix} j_1 t'_1 + j_4 t'_2 & j_2 t'_1 + j_5 t'_2 & j_3 & 0 \\ j_1 t'_4 + j_4 t'_5 & j_2 t'_4 + j_5 t'_5 & 0 & j_3 \end{pmatrix} \quad \text{and} \tag{14}$$

$$\mathbf{J}_{\mathtt{H}\mathtt{T}^{-1},\mathtt{T}\mathbf{x},\mathbf{x}'} = \begin{pmatrix} \frac{-j_2 t_4 + j_1 t_5}{t_1 t_5 - t_4 t_2} & \frac{j_2 t_1 - j_1 t_2}{t_1 t_5 - t_4 t_2} & j_3 & 0 \\ \frac{-j_5 t_4 + j_4 t_5}{t_1 t_5 - t_4 t_2} & \frac{j_5 t_1 - j_4 t_2}{t_1 t_5 - t_4 t_2} & 0 & j_3 \end{pmatrix}. \tag{15}$$

From Eqs. (14) and (15) it follows, that the transformed Jacobian can be expressed as a function of the original Jacobian $\mathbf{J}$ and the affine transformations $\mathtt{T}$ and $\mathtt{T}'$. The proposition is a straightforward consequence of this fact. □

Proposition 3. *Sampson's error measure is invariant to the choice of Cartesian coordinate system, i.e., any rotation or translation of the images does not affect it.*

Proof. From its definition, the affine approximation $A_{\mathtt{H}}$ of $\mathtt{H}$ has the same Jacobian in the measured point $\mathbf{X}$ as $\mathtt{H}$. From Proposition 2 the Jacobians $\mathbf{J}_{\mathtt{T}'\mathtt{H}\mathtt{T}^{-1},\mathtt{T}\mathbf{x},\mathtt{T}'\mathbf{x}'} \sim \mathbf{J}_{\mathtt{T}'\mathbf{A}_{\mathtt{H}}\mathtt{T}^{-1},\mathtt{T}\mathbf{x},\mathtt{T}'\mathbf{x}'}$ for any affine transformations $\mathtt{T}$ and $\mathtt{T}'$. The composition of affine transformations $\mathtt{T}'A_{\mathtt{H}}\mathtt{T}^{-1}$ is an affine transformation, hence

$$A_{\mathtt{T}'\mathtt{H}\mathtt{T}^{-1}} = \mathtt{T}'A_{\mathtt{H}}\mathtt{T}^{-1}. \tag{16}$$

Both rotation and translation fall into the family of affine transformations and so the Eq. (16) holds for any choice of Cartesian coordinates. Sampson's error is then a geometric error for $A_{\mathtt{T}'\mathtt{H}\mathtt{T}^{-1}}$, which we already know is invariant to the choice of Cartesian coordinate system. □

Note that a general affine transformation does preserve neither the geometric nor Sampson's error, since it does not preserve perpendicularity and distances. However, Sampson's error changes in the same manner as the geometric error does, because it is the geometric error of the affine approximation $A_{\mathtt{H}}$ of $\mathtt{H}$ that is covariant to affine transformations of images.

6. Experiments

From Section 5, we already know, that Sampson's and the geometric error are equivalent for pure affine transformations. The aim of this experiment is to show their behavior with respect to the influence of the non-affine part of a general homography $\mathtt{H}$.

Consider now the decomposition $\mathtt{H} = \mathtt{PA}$, where $\mathtt{A}$ is an affine transformation and $\mathtt{P}$ has the form

$$\mathtt{P} = \begin{pmatrix} 1 & 0 & 0 \\ 0 & 1 & 0 \\ p_7 & p_8 & 1 \end{pmatrix}.$$

Let the decomposition $\mathtt{H} = \mathtt{PA}$ exist. Let also $\mathtt{P}' = \mathtt{PT}$ be of the same form as $\mathtt{P}$ and let $\mathtt{A}' = \mathtt{T}^{-1}\mathtt{A}$ be an affine transformation. Then it can be easily shown that if $\mathtt{H} = \mathtt{P}'\mathtt{A}'$ then $\mathtt{T}$ must be the identity to keep both $\mathtt{A}'$ affine and $\mathtt{P}'$ in the desired form. Hence, if such a decomposition exists then it is unique. Let $\mathtt{G} = \mathtt{H}^{-1}$. Then from $\mathtt{H}^{-1}\mathtt{P} = \mathtt{GP} = \mathtt{A}^{-1}$ we get the equations for p_7 and p_8 as

$$p_7 = -\frac{g_7}{g_9} \quad \text{and} \quad p_8 = -\frac{g_8}{g_9}.$$

Thus, the decomposition exists iff $g_9 \neq 0$. The geometric meaning of this condition is that the origin of the coordinate system of the second image does not lie on the image of the line at infinity of the first image, i.e., $(\mathtt{H}^{-\mathtt{T}} l_\infty)^{\mathtt{T}} (0,0,1)^{\mathtt{T}} \neq 0$.

To acquire real data, we shot two images of a checkerboard, see Fig. 3. We manually selected four corresponding points in each image. The four points form rectangles R and R' that are depicted in solid line in Figs. 3A and B, respectively. From these four point-to-point correspondences the homography $\mathtt{H}$ was calculated. The origin of the coordinate system was chosen to coincide with one of the corners and is depicted by the 'X' marker. The homography $\mathtt{H}$ was decomposed into $\mathtt{H} = \mathtt{PA}$. The dashed rectangle in Fig. 3B is the rectangle R mapped from the first image to the second by the affine part $\mathtt{A}$ of $\mathtt{H}$. The dashed line in Fig. 3A arose as a mapping of the dashed rectangle in the second image back to the first by $\mathtt{H}^{-1}$, i.e., the image of R by $\mathtt{H}^{-1}\mathtt{A}$ within the first image.

In this experiment, we will use the following notation: $\mathbf{x}$ and $\mathbf{x}'$ stand for noise-free points, i.e., $\mathbf{x}' \sim \mathtt{H}\mathbf{x}$; $\mathbf{x}_0$ and $\mathbf{x}'_0$ denote the noisy points. The points, where the geometric error is minimized are $\hat{\mathbf{x}}$ and $\hat{\mathbf{x}}'$, and points where Sampson's error is minimized are $\mathbf{x}_{\mathrm{S}}$ and $\mathbf{x}'_{\mathrm{S}}$. Note that $\hat{\mathbf{x}}' \sim \mathtt{H}\hat{\mathbf{x}}$, but $\mathbf{x}'_{\mathrm{S}} \nsim \mathtt{H}\mathbf{x}_{\mathrm{S}}$ in general. In our experiment, we measured different errors: $d_\perp$ and d_{S} are the geometric and Sampson's errors

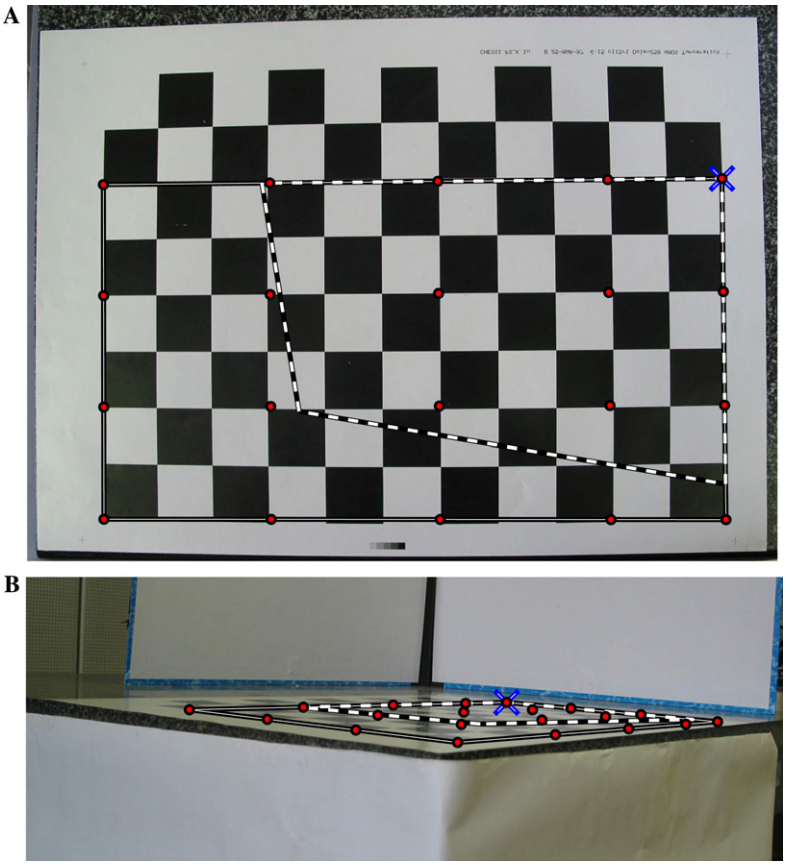

Fig. 3. Experimental setup. Two images of a checkerboard taken by a digital camera. The homography H was estimated from four point-to-point correspondences, shown as corners of the solid-line rectangles. The dashed rectangles show the effect of the affine part of the decomposed H. The origin of the decomposition is depicted by the 'X' marker.

respectively, $d_{\perp}^{*} = \sqrt{d^2(\mathbf{x}, \tilde{\mathbf{x}}) + d^2(\mathbf{x}', \tilde{\mathbf{x}}')}$, similarly $d_{\mathrm{S}}^{*} = \sqrt{d^2(\mathbf{x}, \mathbf{x}_{\mathrm{S}}) + d^2(\mathbf{x}', \mathbf{x}_{\mathrm{S}}')}$. The displacement of points $\mathbf{x}_{\mathrm{S}}$ and $\mathbf{x}_{\mathrm{S}}'$ is measured either as the distance in the second image $d_2(\mathbf{x}_{\mathrm{S}}, \mathbf{x}_{\mathrm{S}}') = d(\mathtt{H}\mathbf{x}_{\mathrm{S}}, \mathbf{x}_{\mathrm{S}}')$ or by using the geometric error $d_{\perp}(\mathbf{x}_{\mathrm{S}}, \mathbf{x}_{\mathrm{S}}')$. The errors were measured at points depicted in Figs. 3A and B. A Gaussian noise with $\sigma = 0.3$ was added to each coordinate of a noise-free point correspondence. All values were obtained as averages over all points over 1010 realizations of noise and are shown in Fig. 4.

The graphs in Fig. 4 show that the geometric (A,B) and Sampson's (C,D) error provide very similar results independently of the value of the non-affine part of the planar homography. The same graphs show that the realization of the noise has a much stronger influence than the values of p_7 and p_8 on both types of the error. The value of σ of the Gaussian noise was set to $\sigma = 0.3$ in this experiment. We observed the same behavior for $\sigma \in \langle 10^{-4}, 10 \rangle$. Graphs E and F show that the displace-

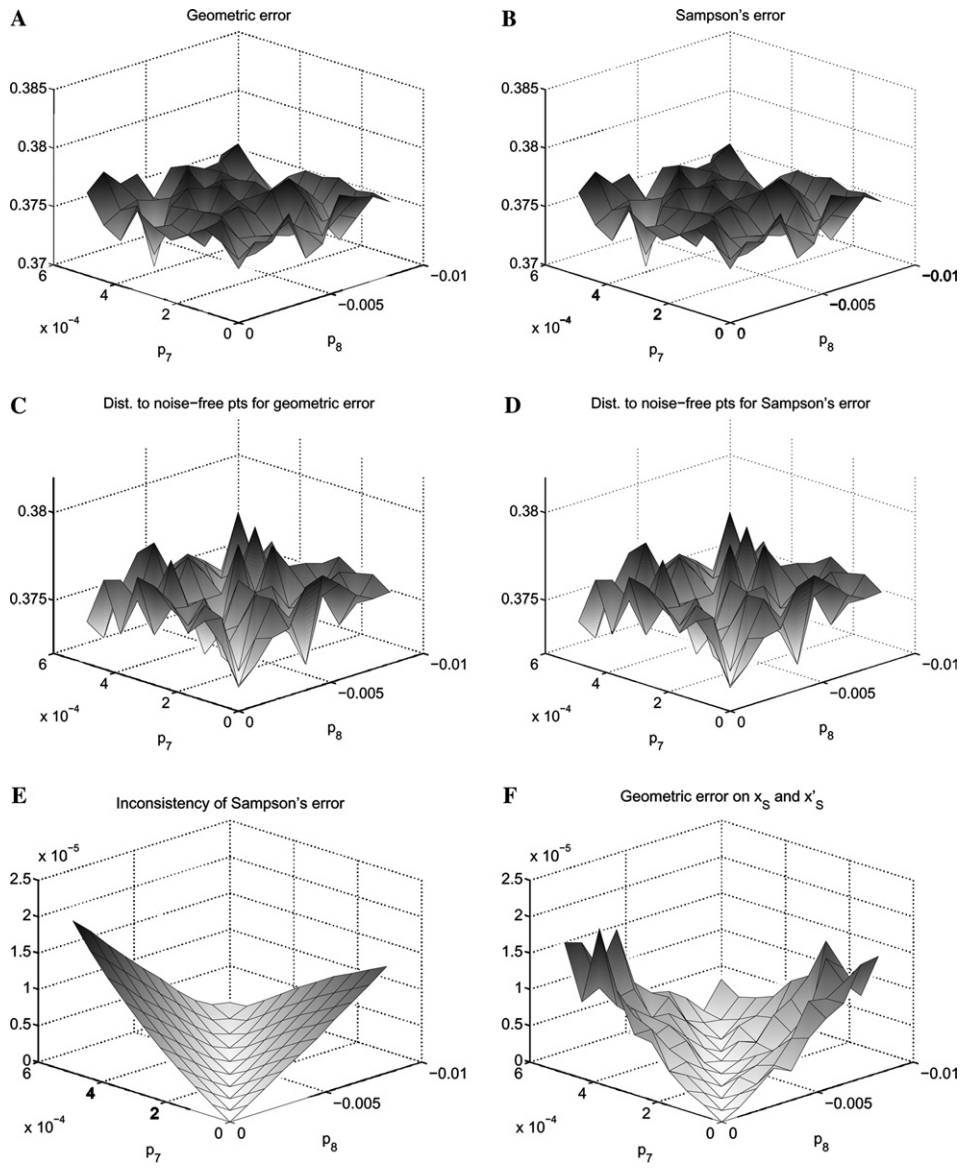

Fig. 4. Dependency of: (A) $d_{\perp}$, (B) d_{S}, (C) $d_{\perp}^{*}$, (D) d_{S}^{*}, (E) $d(\mathtt{H}\mathbf{x}_{\mathrm{S}}, \mathbf{x}'_{\mathrm{S}})$, and (F) $d_{\perp}(\mathbf{x}_{\mathrm{S}}, \mathbf{x}'_{\mathrm{S}})$ on the non-affine part of the homography $\mathtt{H}$.

ment of the points where the Sampson's error is minimized, i.e., $\mathbf{x}_{\mathrm{S}}$ and $\mathbf{x}'_{\mathrm{S}}$, depends on the value of p_7 and p_8. The more the homography "squeezes" the image, the more displaced the points are. On the other hand, the displacement is in four orders of magnitude smaller than the error itself.

The main conclusion of the experiment conducted in this section is that Sampson's error gives sufficiently good results in 2D that are comparable with the geometric error. The displacement of points $\mathbf{x}_S$ and $\mathbf{x}'_S$ is small, but still significantly higher than machine precision and can cause problems while reconstructing 3D points (see Section 7).

7. Triangulation

The method presented in this paper would be useful in applications where a high accuracy is desired. In this section, we will mention one problem where we can use the geometric error for homographies to improve the accuracy of the reconstruction of planes in the scene. We call it *planar triangulation*. It is an extension of the triangulation problem [6].

The two rays in space, the first one from camera center $\mathbf{C}$ through image point $\mathbf{x}$ in the first image and the other one from $\mathbf{C}'$ through $\mathbf{x}'$, will intersect only if $\mathbf{x}'^{\mathrm{T}}\mathbb{F}\mathbf{x} = 0$. If noise is attached to the image coordinates, then the rays may not meet.

In the triangulation problem [6], it is assumed that the fundamental matrix $\mathbb{F}$ is known exactly. For this fundamental matrix, the points $\tilde{\mathbf{x}}$ and $\tilde{\mathbf{x}}'$ are found, so that $\tilde{\mathbf{x}}'^{\mathrm{T}}\mathbb{F}\tilde{\mathbf{x}} = 0$ and the sum of the square distances $d(\mathbf{x}, \tilde{\mathbf{x}})^2 + d(\mathbf{x}', \tilde{\mathbf{x}}')^2$ is minimal.

Assume there is a (dominant) plane in the scene and $\mathtt{H}$ is the homography induced by this plane. When the triangulation method [6] is used, the additional constraint of the planarity is omitted and the reconstructed points will in general not lie in a single plane. The homography $\mathtt{H}$ is compatible [10, Section 12] with the fundamental matrix if, and only if for all $\hat{\mathbf{x}}$

$$(\mathtt{H}\hat{\mathbf{x}})^{\mathrm{T}}\mathbb{F}\hat{\mathbf{x}} = 0.$$

This means all the correspondences satisfying $\hat{\mathbf{x}}' \sim \mathtt{H}\hat{\mathbf{x}}$ will automatically satisfy the epipolar geometry $\hat{\mathbf{x}}'^{\mathrm{T}}\mathbb{F}\hat{\mathbf{x}} = 0$ and hence the two rays in space, passing through $\mathbf{x}$ and $\mathbf{x}'$, respectively, will intersect. Moreover all these intersections in space given by correspondences satisfying homography $\mathtt{H}$ lie on the plane inducing $\mathtt{H}$.

7.1. Experiment

We have made synthetic experiments with the planar triangulation using images of an artificial scene (Figs. 5A and B). From noise-free images we obtained the fundamental matrix $\mathbb{F}$ and the homography $\mathtt{H}$. For testing purposes we used only the points on the front face of the building. Then, we added Gaussian noise with standard deviation σ to the image coordinates. From these noisy points we calculated corrected points using the standard and the planar triangulation. Fig. 5 gives the comparison of the distance of corrected points to the original noise-free points, denoted as 2D error (in pixels), and its standard deviation—graphs C and D. We then computed a 3D reconstruction using the corrected points (both from the standard and the planar triangulation). The distance of reconstructed 3D points to the

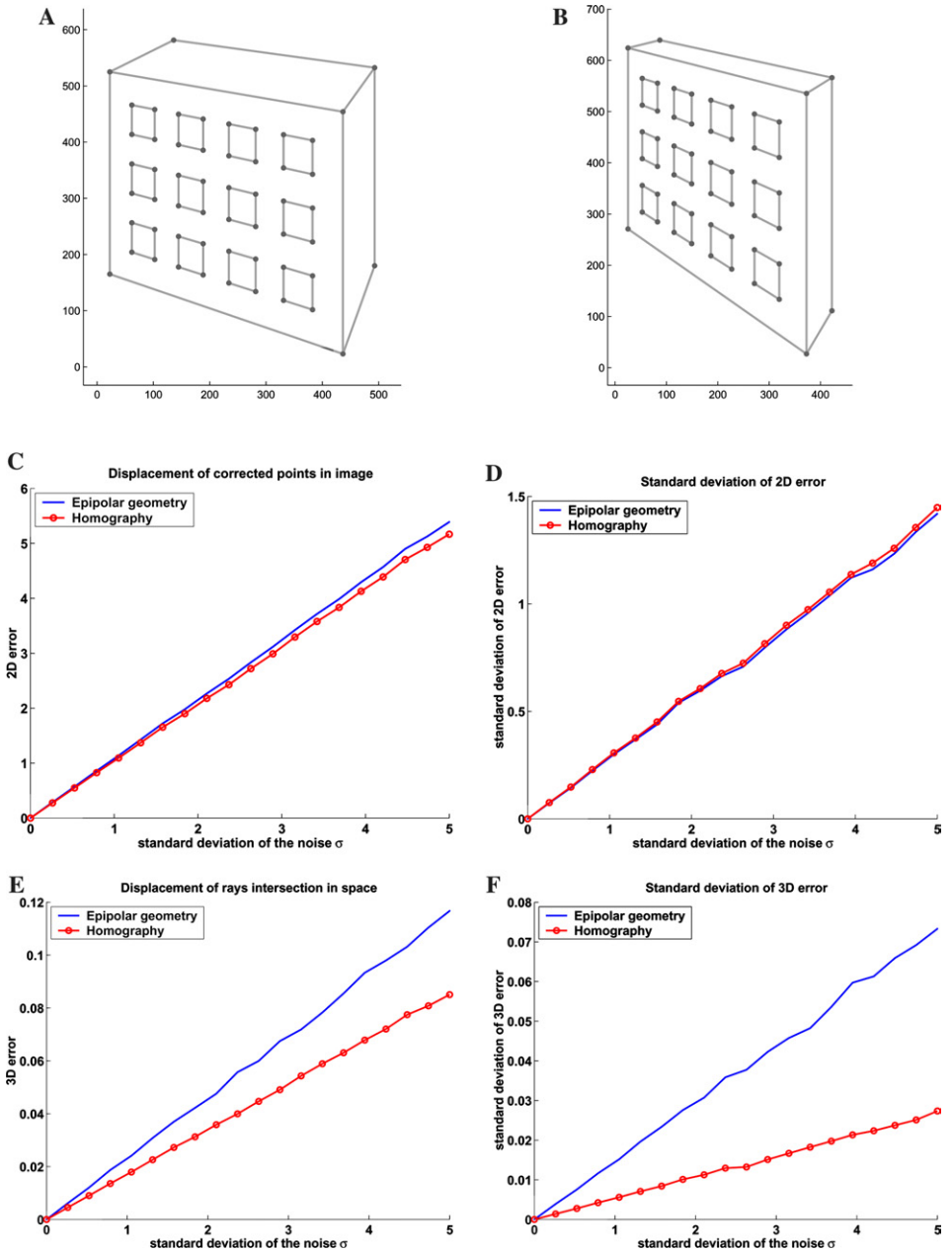

Fig. 5. Synthetic experiment with images (A) and (B). The graphs compare errors in triangulation using the fundamental matrix $\mathtt{F}$ (standard) and the homography $\mathtt{H}$ (planar) in images (C) and (D) and in 3D space (E) and (F). For testing, only points lying in the plane of the frontal side of the building were used. The dimensions of the building are $9 \times 7 \times 1$ units.

original 3D points is denoted as 3D-error (in units, the building dimensions are $9 \times 7 \times 1$)—graphs E and F.

The result of this experiment shows that the decrease in the 2D error is not significant. On the other hand, the 3D error is considerably decreased by the planar triangulation.

When we tried to use Sampson's approximation followed by the standard triangulation (it consists of computing pseudo-inversion and solving a polynomial of degree six), we got similar results to those when using the planar triangulation.

The experiment shows that the accuracy of the reconstruction of a planar scene could be improved by using the planar triangulation instead of the standard one. Using Sampson's approximation together with the standard triangulation gives very similar results as the planar triangulation but it is computationally more expensive and the planarity of the reconstructed scene is not guaranteed.

8. Conclusions

In this paper, a new method for computing the geometric error for homography was introduced. The main contribution of the paper is the derivation of the formula for computing the error. This formula has not been known before. It is interesting to see that the error is obtained as a solution of a degree eight polynomial. We have also proved that there indeed exist a corrected correspondence that minimizes the geometric distance to the measured correspondence, and that the proposed method finds it correctly.

We tested two different methods of measuring correspondence error with respect to given homography $\mathtt{H}$, the geometric error by the Sampson's error. Our experiments had shown that the Sampson's error is sufficiently precise for a wide range of applications including RANSAC. We also discovered (and proved) nice properties of the Sampson's error with respect to affine transformations of images. The applications where the use of the geometric error could bring higher accuracy were shown. This statement is encouraged with experiments with the planar triangulation.

Appendix A. Proof of correctness

Proposition 4. *Let* $\mathtt{H}$ *be a regular matrix of the following form*:

$$\mathtt{H} = \begin{pmatrix} h_1 & h_2 & h_3 \\ h_4 & h_5 & h_6 \\ h_7 & 0 & h_9 \end{pmatrix}.$$

Then the function

$$e = x^2 + y^2 + \left(\frac{x'}{w'}\right)^2 + \left(\frac{y'}{w'}\right)^2, \tag{A.1}$$

where

$$x' = h_1 x + h_2 y + h_3, \tag{A.2}$$

$$y' = h_4 x + h_5 y + h_6, \tag{A.3}$$

$$w' = h_7 x + h_9 \tag{A.4}$$

has a global minimum. In this minimum the partial derivatives of e are defined and equal to zero.

Proof. First of all we introduce the notation used throughout the proof. Let us write e as a sum of three functions $e_1 = x^2 + y^2$, $e_2 = (x'/w')^2$, and $e_3 = (y'/w')^2$, i.e., $e = e_1 + e_2 + e_3$. Since all e_i, $i \in \{1, 2, 3\}$, are nonnegative, we have $e \geqslant e_i$. We can also define three lines, $\ell_{\mathbf{x}'}$, $\ell_{\mathbf{y}'}$, and $\ell_{\mathbf{w}'}$ in $\mathbb{R}^2$ letting x', y', and w' equal zero in (A.2), (A.3), and (A.4), respectively. Let **A** be the point of intersection of $\ell_{\mathbf{w}'}$ with $\ell_{\mathbf{x}'}$ and **B** be the point where $\ell_{\mathbf{w}'}$ intersects $\ell_{\mathbf{y}'}$. Since $\mathtt{H}$ is regular, there does not exist any $\mathbf{x} = (x, y, 1)^{\mathtt{T}}$, so that $\mathtt{H}\mathbf{x} = \mathbf{0}$. Thus **A** and **B** are two different points. The situation is depicted in the Fig. 6.

The function e is continuous and even differentiable throughout the region where the denominator $h_7 x + h_9$ is nonzero and finite, i.e., in $\mathbb{R}^2 \setminus \ell_{\mathbf{w}'}$. The term e_1 tends to plus infinity in all points of $\ell_{\mathbf{w}'}$ except for **A** where it is guaranteed to be nonnegative. Analogously, the term e_2 tends to plus infinity in all points of $\ell_{\mathbf{w}'}$ except for **B** where it is guaranteed to be nonnegative. The sum of e_1 and e_2, and thus e, tends to plus infinity in all points of $\ell_{\mathbf{w}'}$.

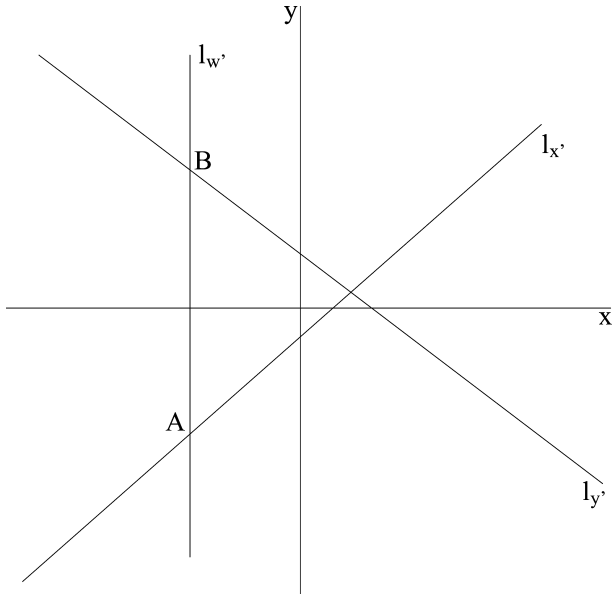

Fig. 6. Lines $\ell_{\mathbf{x}'}$, $\ell_{\mathbf{y}'}$, and $\ell_{\mathbf{w}'}$ are sets of points, where $x' = 0$, $y' = 0$, and $w' = 0$, respectively.

We choose a point in $\mathbb{R}^2 \setminus \ell_{\mathbf{w}'}$ and take the value of e in it for a constant K. The set

$$I = \{(x, y) \in \mathbb{R}^2 \setminus \ell_{\mathbf{w}'} \mid e(x, y) \leqslant K\}$$

is nonempty and closed. It is also bounded because it is a subset of the circle

$$\{(x, y) \in \mathbb{R}^2 \mid x^2 + y^2 \leqslant K\}.$$

Therefore I is a compact set and so it contains all global minima of e. At least one global minimum of e exists because the values of e on I are images of a compact set under a continuous mapping, thus they form a compact subset of $\mathbb{R}$. □

Appendix B. Coefficients of the polynomial

In Section 3, we derived the formula for computing the geometric error. Here we focus on the implementation.

First of all we can see that the image rotation matrix $\mathtt{R}$ depends only on h_7 and h_8 (10). From (8) we know that $\mathtt{R}$ stays unchanged by the translations $\mathtt{L}$ and $\mathtt{L}'$. So the matrix $\mathtt{R}$ could be computed directly from $\mathtt{H}$. Matrix $\mathtt{R}$ is the same for all the correspondences.

Coefficients of the resulting polynomial of degree eight are sums of products of entries of the matrix $\mathtt{Q}$, which are quite complicated. We can apply image rotation matrix $\mathtt{R}'$ to the second image. We have

$$\mathtt{R}'\tilde{\mathbf{x}}' = \mathtt{R}'\mathtt{Q}\tilde{\mathbf{x}},$$

and $\mathtt{Q}' = \mathtt{R}'\mathtt{Q}$. To decrease the number of summands, we can design this rotation in the same way as the matrix $\mathtt{R}$ to make $q'_4 = 0$. Note, that q'_8 stays unchanged by the rotation $\mathtt{R}'$, so $q'_8 = q_8 = 0$. Matrix $\mathtt{R}'$ differs for each correspondence.

After applying the rotations on both images, we have homography $\bar{Q}$ in the form

$$\bar{Q} = \begin{pmatrix} \bar{q}_1 & \bar{q}_2 & \bar{q}_3 \\ 0 & \bar{q}_5 & \bar{q}_6 \\ \bar{q}_7 & 0 & \bar{q}_9 \end{pmatrix}.$$

The resulting polynomial is in the following form:

$$\sum_{i=0}^{8} \bar{p}_i \tilde{x}^i.$$

Here is the list of the coefficients p_i expressed in entries $\bar{q}$ of the matrix $\bar{Q}$. We use the following substitutions:

$$t = \bar{q}_3\bar{q}_5 - \bar{q}_2\bar{q}_6,$$
$$r = \bar{q}_2^2 + \bar{q}_5^2 + \bar{q}_9^2.$$

The polynomial coefficients are:

$$\bar{p}_0 = \bar{q}_9^3((-\bar{q}_3^2 - \bar{q}_6^2)\bar{q}_7\bar{q}_9 + \bar{q}_1\bar{q}_3 r) + \bar{q}_1\bar{q}_5\bar{q}_9 rt - \bar{q}_7(\bar{q}_9^2 + r)t^2,$$

$$\begin{aligned}\bar{p}_1 = & -4\bar{q}_3^2\bar{q}_7^2\bar{q}_9^3 - 4\bar{q}_6^2\bar{q}_7^2\bar{q}_9^3 + 3\bar{q}_1\bar{q}_3\bar{q}_7\bar{q}_9^2 r + \bar{q}_9 r(\bar{q}_1^2(\bar{q}_5^2 + \bar{q}_9^2) + \bar{q}_9^2 r) \\ & - \bar{q}_1\bar{q}_5\bar{q}_7 rt - 4\bar{q}_7^2\bar{q}_9 t^2,\end{aligned}$$

$$\begin{aligned}\bar{p}_2 = & \bar{q}_7(\bar{q}_9(-6(\bar{q}_3^2 + \bar{q}_6^2)\bar{q}_7^2\bar{q}_9 - \bar{q}_1\bar{q}_3\bar{q}_7(\bar{q}_9^2 - 3r) + 4\bar{q}_9^3 r + 3\bar{q}_9 r^2 \\ & + \bar{q}_1^2\bar{q}_9(\bar{q}_5^2 + \bar{q}_9^2 + 3r)) - 5\bar{q}_1\bar{q}_5\bar{q}_7\bar{q}_9 t - 2\bar{q}_7^2 t^2),\end{aligned}$$

$$\begin{aligned}\bar{p}_3 = & \bar{q}_7^2(\bar{q}_9(-4(\bar{q}_3^2 + \bar{q}_6^2)\bar{q}_7^2 + 4\bar{q}_9^4 + 14\bar{q}_9^2 r + 3r^2) + \bar{q}_1^2(-(\bar{q}_5^2\bar{q}_9) + 3\bar{q}_9(\bar{q}_9^2 + r)) \\ & + \bar{q}_1\bar{q}_7(\bar{q}_3(-3\bar{q}_9^2 + r) - 3\bar{q}_5 t)),\end{aligned}$$

$$\bar{p}_4 = \bar{q}_7^3((-\bar{q}_3^2 - \bar{q}_6^2)\bar{q}_7^2 - 3\bar{q}_1\bar{q}_3\bar{q}_7\bar{q}_9 + 16\bar{q}_9^4 + 18\bar{q}_9^2 r + r^2 + \bar{q}_1^2(-\bar{q}_5^2 + 3\bar{q}_9^2 + r)),$$

$$\bar{p}_5 = \bar{q}_7^4(-(\bar{q}_1\bar{q}_3\bar{q}_7) + \bar{q}_1^2\bar{q}_9 + 25\bar{q}_9^3 + 10\bar{q}_9 r),$$

$$\bar{p}_6 = \bar{q}_7^5(19\bar{q}_9^2 + 2r),$$

$$\bar{p}_7 = 7\bar{q}_7^6\bar{q}_9,$$

$$\bar{p}_8 = \bar{q}_7^7.$$

References

[1] Y. Kanazawa, K. Kanatani, Stabilizing image mosaicing by model selection, in: Proc. Second Workshop on 3D Structure from Multiple Images of Large-scale Environments and Applications to Virtual and Augmented Reality, 2000, pp. 10–17.
[2] P. Pritchett, A. Zisserman, Wide baseline stereo matching, in: Proc. Internat. Conf. Computer Vision, 1998, pp. 754–760.
[3] J. Matas, O. Chum, M. Urban, T. Pajdla, Robust wide baseline stereo from maximally stable extremal regions, in: Proc. British Machine Vision Conf., vol. 1, BMVA, London, UK, 2002, pp. 384–393.
[4] M.A. Fischler, R.C. Bolles, Random sample consensus: a paradigm for model fitting with applications to image analysis and automated cartography, Commun. ACM 24 (6) (1981) 381–395.
[5] K. Kanatani, Statistical Optimization for Geometric Computation: Theory and Practice, vol. 18 of Machine Intelligence and Pattern Recognition, Elsevier, Amsterdam, 1996.
[6] R.I. Hartley, P. Sturm, Triangulation, Comput. Vision Image Und. 2 (68) (1997) 146–157.
[7] P. Sturm, Vision 3D non calibrée—contributions à la reconstruction projective et étude des mouvements critiques pour l'auto-calibrage, Ph.D. Thesis, INPG, Grenoble, France, 1997.
[8] O. Chum, The reconstruction of 3D scene from the correspondences in images, Master's Thesis, MFF UK, Prague, Czech Republic, January 2001.
[9] O. Chum, T. Pajdla, Evaluating error of homography, in: Proc. Computer Vision Winter Workshop, Wien, Austria, 2002, pp. 315–324.
[10] R.I. Hartley, A. Zisserman, Multiple View Geometry in Computer Vision, Cambridge University Press, Cambridge, UK, 2000.
[11] P.D. Sampson, Fitting conic sections to very scattered data: An iterative refinement of the Bookstein algorithm, Comput Graph. Image Process. 18 (1982) 97–108.
[12] Waterloo Maple Inc., Maple V, http://www.maplesoft.com.